

REPORT DOCUMENTATION PAGE			Form Approved OMB NO. 0704-0188		
<p>The public reporting burden for this collection of information is estimated to average 1 hour per response, including the time for reviewing instructions, searching existing data sources, gathering and maintaining the data needed, and completing and reviewing the collection of information. Send comments regarding this burden estimate or any other aspect of this collection of information, including suggestions for reducing this burden, to Washington Headquarters Services, Directorate for Information Operations and Reports, 1215 Jefferson Davis Highway, Suite 1204, Arlington VA, 22202-4302. Respondents should be aware that notwithstanding any other provision of law, no person shall be subject to any penalty for failing to comply with a collection of information if it does not display a currently valid OMB control number. PLEASE DO NOT RETURN YOUR FORM TO THE ABOVE ADDRESS.</p>					
1. REPORT DATE (DD-MM-YYYY)		2. REPORT TYPE Technical Report		3. DATES COVERED (From - To) -	
4. TITLE AND SUBTITLE DFT Study of BZY Cluster Model			5a. CONTRACT NUMBER W911NF-13-1-0158		
			5b. GRANT NUMBER		
			5c. PROGRAM ELEMENT NUMBER 206022		
6. AUTHORS Changyong Qin			5d. PROJECT NUMBER		
			5e. TASK NUMBER		
			5f. WORK UNIT NUMBER		
7. PERFORMING ORGANIZATION NAMES AND ADDRESSES Benedict College Office of Research 1600 Harden St. Columbia, SC 29204 -1058			8. PERFORMING ORGANIZATION REPORT NUMBER		
9. SPONSORING/MONITORING AGENCY NAME(S) AND ADDRESS (ES) U.S. Army Research Office P.O. Box 12211 Research Triangle Park, NC 27709-2211			10. SPONSOR/MONITOR'S ACRONYM(S) ARO		
			11. SPONSOR/MONITOR'S REPORT NUMBER(S) 62940-CH-REP.8		
12. DISTRIBUTION AVAILABILITY STATEMENT Approved for public release; distribution is unlimited.					
13. SUPPLEMENTARY NOTES The views, opinions and/or findings contained in this report are those of the author(s) and should not be construed as an official Department of the Army position, policy or decision, unless so designated by other documentation.					
14. ABSTRACT Technical report for 2013-2014 (DFT modeling part)					
15. SUBJECT TERMS DFT, BZY, Cluster Model, Modeling					
16. SECURITY CLASSIFICATION OF:		17. LIMITATION OF ABSTRACT UU	15. NUMBER OF PAGES	19a. NAME OF RESPONSIBLE PERSON Changyong Qin	
a. REPORT UU	b. ABSTRACT UU			c. THIS PAGE UU	19b. TELEPHONE NUMBER 803-705-4582

## **Report Title**

DFT Study of BZY Cluster Model

## **ABSTRACT**

Technical report for 2013-2014 (DFT modeling part)

# Novel MC/BZY Proton Conductor: Materials Development, Device Evaluation, and Theoretical Exploration using CI and DFT Methods

Changyong Qin, Benedict College, Columbia, SC 29204 (PI)

Kevin Huang, University of South Carolina, Columbia, SC 29208 (Co-PI)

## (DFT Modeling Part)

During this reporting period, our DFT efforts were focused on determining the surface energy of BaZrO<sub>3</sub> perovskite with different surface terminations. We first optimized the bulk structure of BaZrO<sub>3</sub> perovskite. Second, we cleaved the low index surface, namely {100}, {110} and {111} surfaces, and examined the stability of these surfaces by evaluating their surface energies. Third, we selected the most stable surface as the basis for constructing the super-surface, and then introduced the pairs of Y atoms and oxygen vacancies (one vacancy for each pair of Y) to build the surface of BaZr<sub>0.8</sub>Y<sub>0.2</sub>O<sub>3-δ</sub>. In the next reporting period, we will introduce the OH<sup>-</sup> and CO<sub>3</sub><sup>2-</sup> to the super-surface to simulate the proton conducting behaviors at the interface between BaZr<sub>0.8</sub>Y<sub>0.2</sub>O<sub>3-δ</sub> and carbonate.

### I. The structural features of BaZrO<sub>3</sub> perovskite

The BaZrO<sub>3</sub> ceramic has an ideal cubic perovskite structure with a space group (Pm3m) and point-group symmetry (*O<sub>h</sub>*). As shown in Figure 1, the barium atoms sit at the corners of a simple cubic unit cell, the oxygen atoms sit on the faces and the zirconium atom sits at the center. Moreover, Zr atoms are bonded to six O atoms which form an octahedral ZrO<sub>6</sub> while the Ba atoms are bonded to twelve O atoms with a cuboctahedral configuration which forms BaO<sub>12</sub> cluster.

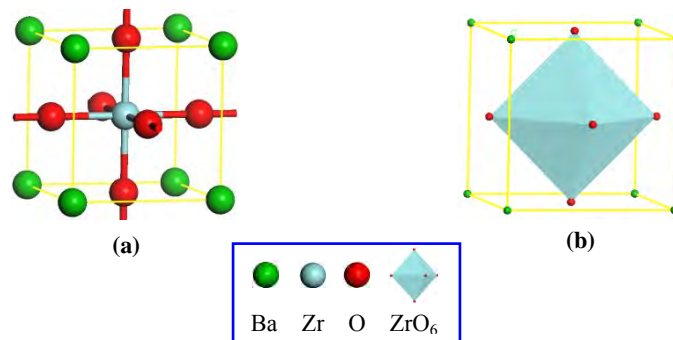


Figure 1. Crystal structure of BaZrO<sub>3</sub> showing (a) atomic positions of the unit cell and (b) structure depicting by ZrO<sub>6</sub> octahedra.

### II. The parameters test and relaxation of BaZrO<sub>3</sub> structure

First, we tested the calculated parameters in our DFT model. It should be mentioned that the convergence of the cutoff energy, the number of *k*-points, and the size of the vacuum layer has been carefully checked. For all the calculations, we have used the VASP *ab initio* package [Phys. Rev. B 54:11169-11186, 1996], and the PBE functional [Phys. Rev. Lett. 77:3865, 1996] has been

employed. A cutoff energy of 500 eV and a  $6 \times 6 \times 6$  Monkhorst-Pack k-point mesh [Phys. Rev. B 13:5188-5192, 1976] for  $1 \times 1 \times 1$  unit cell have been determined. Spin-polarized calculations have been applied throughout. The  $2s^2 2p^4$  of O,  $4s^2 4p^6 5s^2 4d^2$  of Zr and  $5s^2 5p^6 6s^2$  of Ba were treated as valence electrons in the DFT calculations. For optimization of the atomic structure, the Hellmann-Feynman forces have been minimized to the maximum value of 0.02 eV/Å on each atom of the system.

To test the reliability of our theoretical level and parameters as mentioned above, the unit cell parameters, ion positions and electronic structures of the cubic  $\text{BaZrO}_3$  were first calculated at the concerned levels, allowing both unit cell parameters and atomic positions to relax. Our optimized the lattice constant of  $\text{BaZrO}_3$  is 4.25 Å, which is in good agreement with the experimental value of 4.20 Å [Dalton Trans. 3061–3066, 2004; New Physics: Sae Mulli, 63(8):939-944,2013] and the theoretical value of 4.24 Å [Phys. Rev. B 75: 155431, 2007], with less than 1% deviation in the cell parameters. Figure 2 shows the total density of states (TDOS) and the energy bands structure of the  $\text{BaZrO}_3$ . Our calculated the energy gap of  $\text{BaZrO}_3$  is 2.78 eV, which is slightly smaller than previous value of 3.1 eV [Phys. Rev. B 75: 155431, 2007] and is significantly lower than the experimental value of 4.9 eV [New Physics: Sae Mulli, 63(8):939-944, 2013] or 5.33 eV [Sci. Technol. B 18:1785, 2000]. This difference is quite usual for DFT calculations and can be largely attributed to the underestimation of band gaps by DFT-LDA (local density approximation) or GGA (generalized gradient approximation). Figure 2 indicates that the  $\text{BaZrO}_3$  is a wide band gap semiconductor.

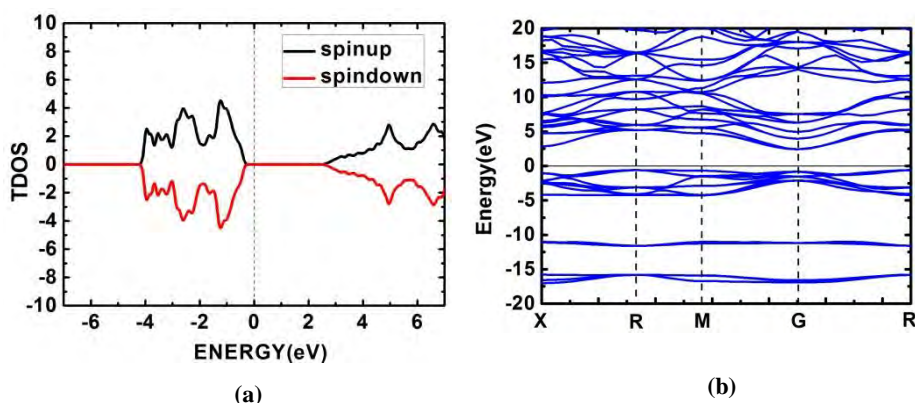


Figure 2. The total density of states (TDOS) of the  $\text{BaZrO}_3$  (a) and the energy bands (b).

### III. The stability of different surface

Second, we calculated the surface energies for different Miller indices in order to examine the stability of different surface for  $\text{BaZrO}_3$ . We have focused our attention on the low index surfaces of cubic  $\text{BaZrO}_3$ , namely  $\{100\}$ ,  $\{110\}$  and  $\{111\}$ . In this part of calculations, a  $2 \times 1$  super-surface and eight atom layers are performed. The vacuum layer of 15 Å has been assembled for our concerned surface relaxations. Cleavage of these three planes leads to two different dipolar surfaces for each Miller index. As a consequence, all the surfaces will have divergent surface energies in the macroscopic limit. However, the dipole and its associated divergent energy can be removed by surface reconstruction. As described in the early literature [J. Mater. Chem. 10:2298-2305, 2000], the simplest reconstruction involves transferring half the ions from one surface to the complementary surfaces. By using this strategy, we constructed the six surfaces and followed the

full optimization for each structure. The surface energy of the  $i$ th surface  $E_i$  has been calculated by

$$E_i = \frac{E_{surf} - E_{bulk}}{2S} \quad (1)$$

Where  $E_{surf}$  and  $E_{bulk}$  are the total energy of the  $i$ th surface and the energy of bulk with the same number of ions, respectively. The  $S$  represents the reconstructed surface.

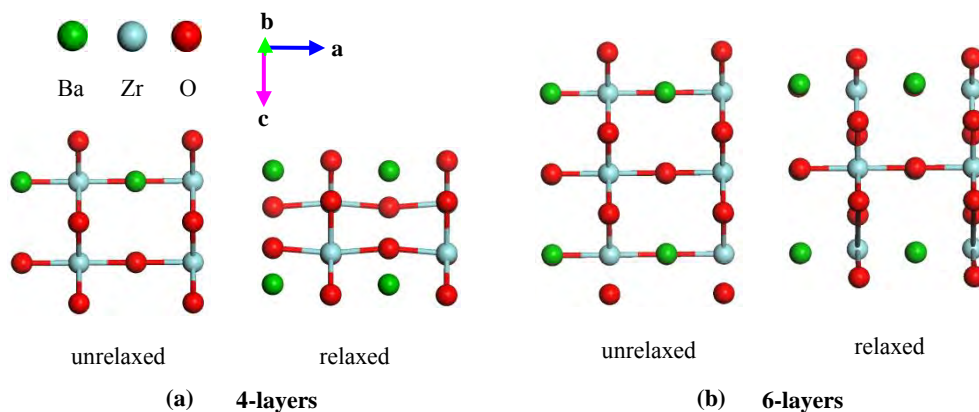
The calculated surface energies for the three surfaces of BaZrO<sub>3</sub> are summarized in Table 1. From the surface energies listed in Table 1, it is predicted that the {100} surfaces will terminate with Ba and O ions, the {110} surface with an oxide layer, and the {111} surface with a Zirconium layer. It is clearly seen that the order of stability for the surfaces of BaZrO<sub>3</sub> is: {110} ≥ {100} > {111}. This trend was also observed in the LaCoO<sub>3</sub> perovskite [J. Mater. Chem. 10:2298-2305, 2000], where the {110} (O-terminating) surface is predicted to be the most stable. Furthermore, our results also suggest that the {110} and {100} surfaces are competitive. The highest stability of {110} agrees with the XRD patterns [Ceramics International 38: 2129–2138, 2012], where the intensity of the {110} peak is the highest.

Table 1. The calculated surface energies for different Miller index of BaZrO<sub>3</sub>.

Miller index	{100}OZr	{100}BaO	{110}O	{110}BaOZr	{111}Zr	{111}BaO <sub>3</sub>
Surface Energy (Jm <sup>-2</sup> )	1.25	1.11	1.10	Non-convergence	1.99	2.30

#### IV. The thickness test of {110}O surface

Next, we took the {110}O and the {100}BaO surface as examples to construct the super-surface. First, the {110}O surface was used as an example to calculation since it has the most stability. Primarily, in order to balance the calculation accuracy and the time cost, we needed to estimate the suitable thickness of the {110}O surface. So, we relaxed the {110}O surface with 4-layers, 6-layers, 8-layers and 10-layers slab, respectively. The structures of unrelaxed and relaxed are displayed in Figure 3. The calculated surface energies as the function of the number of atomic layers are plotted in Figure 4. From the relaxed structures and the surface energy, we found in particular that the 6- or 8-layers slabs are thick enough for simulation of {110}O surface with surface energy convergence.



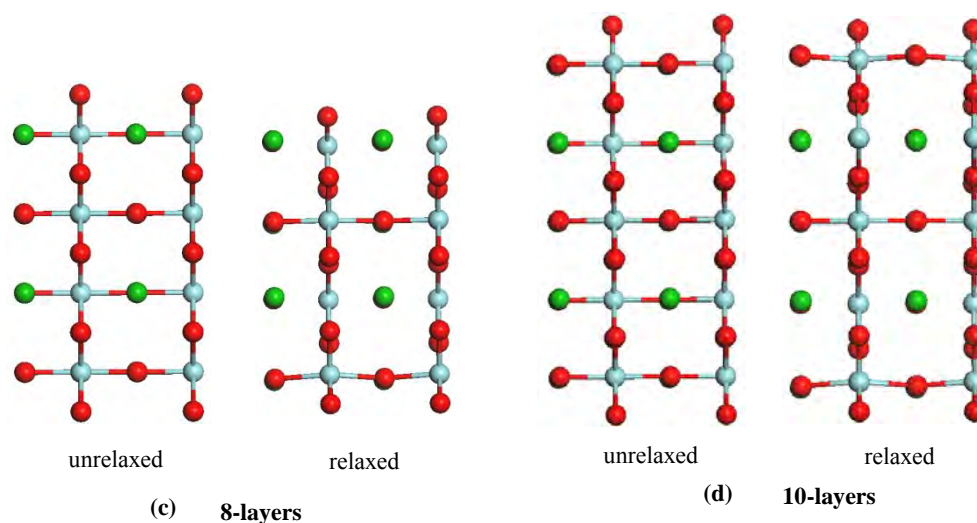


Figure 3. The unrelaxed and relaxed surface structures (side view) for 4-layers (a), 6-layers (b), 8-layers (c) and 10-layers (d) of the  $\{110\}$ O termination surface of the  $\text{BaZrO}_3$ .

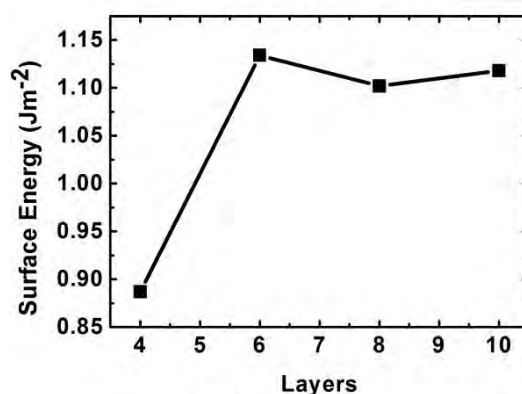


Figure 4. The surface energy as the function of the number of atomic layers.

## V. Future work

In the near future, we will construct the super-surface with the  $\{110\}$  oxygen termination, as shown in Figure 5, where a 7-layers slab terminated on both sides with an oxygen plane will be used. Use of such symmetrical slab permits to avoid a problem of the surface dipole moment.

We will then relax the super-surface of  $\{110\}$ O (structure in Figure 5), introduce the defects by incorporation of pairs of Y atoms and O vacancies (one O vacancy for each pair of Y). In this effort, there will be a few variations, such as O vacancies locate at the surface and subsurface, the distribution of Y atoms in the  $\{110\}$ O slab and so on. Next, we will construct the models of interface between the  $\text{BaZr}_{0.8}\text{Y}_{0.2}\text{O}_{3-\delta}$  and the carbonate by introducing the carbonate ions on the surface. Finally, we will simulate the proton conduction at the interface by introducing the OH<sup>-</sup> group to occupy the oxygen vacancy of a  $\text{BaZr}_{0.8}\text{Y}_{0.2}\text{O}_{3-\delta}$  slab.

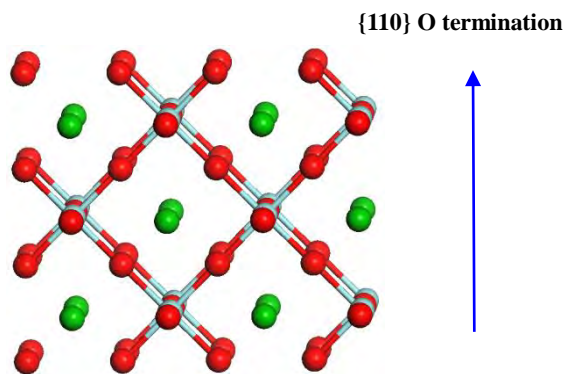


Figure 5. Super-surface of 7-layers {110} oxygen termination.